PDGF-AB and 5-Azacytidine induce conversion of somatic cells into tissue-regenerative multipotent stem cells

Vashe Chandrakanthan[a,b,1], Avani Yeola[a,b], Jair C. Kwan[a,b,2], Rema A. Oliver[b,c], Qiao Qiao[a,b], Young Chan Kang[a,b], Peter Zarzour[a,b], Dominik Beck[a,b], Lies Boelen[a,b,3], Ashwin Unnikrishnan[a,b], Jeanette E. Villanueva[d], Andrea C. Nunez[a,b], Kathy Knezevic[a,b], Cintia Palu[a,b], Rabab Nasrallah[a,b], Michael Carnell[e], Alex Macmillan[e], Renee Whan[e], Yan Yu[b,c], Philip Hardy[f], Shane T. Grey[d], Amadeus Gladbach[g], Fabien Delerue[g], Lars Ittner[g,h], Ralph Mobbs[i], Carl R. Walkley[j,k], Louise E. Purton[j,k], Robyn L. Ward[a,b], Jason W. H. Wong[a,b], Luke B. Hesson[a,b], William Walsh[b,c], and John E. Pimanda[a,b,l,1]

[a]Lowy Cancer Research Centre, University of New South Wales (UNSW) Australia, Sydney, NSW 2052, Australia; [b]The Prince of Wales Clinical School, UNSW Australia, Sydney, NSW 2052, Australia; [c]Surgical and Orthopaedic Research Laboratories, UNSW Australia, Sydney, NSW 2052, Australia; [d]Garvan Institute of Medical Research, Darlinghurst, NSW 2010, Australia; [e]Mark Wainwright Analytical Centre, UNSW Australia, Sydney, NSW 2052, Australia; [f]Cyto Labs Pty. Ltd. Australia, School of Medicine and Pharmacology, University of Western Australia, Fremantle, WA 6102, Australia; [g]Dementia Research Unit, Department of Anatomy, School of Medical Sciences, Faculty of Medicine, University of New South Wales, Sydney, NSW 2052, Australia; [h]Neuroscience Research Australia, Sydney, NSW 2031, Australia; [i]Department of Neurosurgery, The Prince of Wales Hospital, Sydney, NSW 2032, Australia; [j]St. Vincent's Institute of Medical Research, The University of Melbourne, Fitzroy, VIC 3065, Australia; [k]The Department of Medicine, The University of Melbourne, Melbourne, VIC 3010, Australia; and [l]Department of Haematology, The Prince of Wales Hospital, Sydney, NSW 2032, Australia

Edited by Hans Clevers, University Medical Centre Utrecht, Utrecht, The Netherlands, and approved February 29, 2016 (received for review December 1, 2015)

Current approaches in tissue engineering are geared toward generating tissue-specific stem cells. Given the complexity and heterogeneity of tissues, this approach has its limitations. An alternate approach is to induce terminally differentiated cells to dedifferentiate into multipotent proliferative cells with the capacity to regenerate all components of a damaged tissue, a phenomenon used by salamanders to regenerate limbs. 5-Azacytidine (AZA) is a nucleoside analog that is used to treat preleukemic and leukemic blood disorders. AZA is also known to induce cell plasticity. We hypothesized that AZA-induced cell plasticity occurs via a transient multipotent cell state and that concomitant exposure to a receptive growth factor might result in the expansion of a plastic and proliferative population of cells. To this end, we treated lineage-committed cells with AZA and screened a number of different growth factors with known activity in mesenchyme-derived tissues. Here, we report that transient treatment with AZA in combination with platelet-derived growth factor–AB converts primary somatic cells into tissue-regenerative multipotent stem (iMS) cells. iMS cells possess a distinct transcriptome, are immunosuppressive, and demonstrate long-term self-renewal, serial clonogenicity, and multigerm layer differentiation potential. Importantly, unlike mesenchymal stem cells, iMS cells contribute directly to in vivo tissue regeneration in a context-dependent manner and, unlike embryonic or pluripotent stem cells, do not form teratomas. Taken together, this vector-free method of generating iMS cells from primary terminally differentiated cells has significant scope for application in tissue regeneration.

platelet-derived growth factor-AB | 5-Azacytidine | tissue regeneration | multipotent stem cells | cell reprogramming

The goal of regenerative medicine is to reconstitute damaged or defective tissues. A supply of healthy cells capable of contributing to tissue repair and regeneration without risk of host rejection or malignant transformation is vital to achieving this goal. In this regard, bone marrow transplantation and skin and bone grafts have proven clinical utility (1–4). However, for the majority of tissues that require regeneration, harvesting and expanding stem and progenitor cells is a challenge, and tissue grafting is not an option due to site- and tissue-specific limitations. Although mesenchymal stem cells (MSCs) harvested from bone marrow or fat are regularly injected into sites of tissue injury, there is little objective evidence that these cells are retained at sites of injection or contribute directly to new tissue formation (5).

Given the challenges faced in harnessing resident stem cells to regenerate and repair tissues with low baseline turnover, research efforts over many decades have been directed toward converting terminally differentiated cells into stem cells. Somatic cells can be reprogrammed into pluripotent cells by transferring their nuclear contents into oocytes (6), by fusion with ES cells (7, 8), or by introducing defined transcription factors (9). However, as the direct implantation of autologous pluripotent cells runs the risk of ectopic tissue production and malignant transformation, the focus has shifted to reprogram cells directly into specific cell types using defined transcription factors (10). Methods to generate mouse [e.g., neurons (11), pancreatic b cells (12), hepatocyte-like cells

Significance

In this report we describe the generation of tissue-regenerative multipotent stem cells (iMS cells) by treating mature bone and fat cells transiently with a growth factor [platelet-derived growth factor–AB (PDGF-AB)] and 5-Azacytidine, a demethylating compound that is widely used in clinical practice. Unlike primary mesenchymal stem cells, which are used with little objective evidence in clinical practice to promote tissue repair, iMS cells contribute directly to in vivo tissue regeneration in a context-dependent manner without forming tumors. This method can be applied to both mouse and human somatic cells to generate multipotent stem cells and has the potential to transform current approaches in regenerative medicine.

Author contributions: V.C., R.A.O., S.T.G., L.I., R.L.W., L.B.H., W.W., and J.E.P. designed research; V.C., A.Y., J.C.K., R.A.O., Q.Q., Y.C.K., P.Z., D.B., J.E.V., A.C.N., K.K., R.N., Y.Y., P.H., A.G., and F.D. performed research; R.M., C.R.W., and L.E.P. contributed new reagents/analytic tools; V.C., R.A.O., L.B., A.U., J.E.V., C.P., M.C., A.M., R.W., S.T.G., L.I., J.W.H.W., L.B.H., and J.E.P. analyzed data; and V.C. and J.E.P. wrote the paper.

The authors declare no conflict of interest.

This article is a PNAS Direct Submission.

Data deposition: The data reported in this paper have been deposited in the Gene Expression Omnibus (GEO) database, www.ncbi.nlm.nih.gov/geo (accession no. GSE59282).

[1]To whom correspondence may be addressed. Email: jpimanda@unsw.edu.au or v.chandrakanthan@unsw.edu.au.

[2]Present address: Faculty of Medicine, Sydney Medical School, University of Sydney, Sydney, NSW 2006, Australia.

[3]Present address: Section of Immunology, Department of Medicine, Imperial College London, London W2 1PG, United Kingdom.

This article contains supporting information online at www.pnas.org/lookup/suppl/doi:10.1073/pnas.1518244113/-/DCSupplemental.

www.pnas.org/cgi/doi/10.1073/pnas.1518244113

(13), cardiomyocytes (14), and hematopoietic progenitors (15, 16)] and human [e.g., cardiomyocytes (17) and blood progenitors (4)] cells have been reported. However, these methods require vector-based gene transfer and are of low reprogramming efficiency. Moreover, most tissues are a complex mix of different cell types, and there is a need for the generation of autologous stem cells that can directly contribute to repair and regeneration of multiple cell types in a context-dependent manner.

Limb regeneration in salamander species is dependent not on resident stem-cell proliferation but plasticity of differentiated cells where mesenchymal tissues such as cartilage, muscle, and connective tissue underlying the wound epidermis lose their differentiated characteristics and adopt a blastemal cell state (18). The blastema is essentially a zone of mesenchymal cells that proliferate, differentiate, and regenerate the limb according to the predetermined body plan. To replicate the regenerative response in salamanders would require the generation of plastic, proliferative cells from terminally differentiated mammalian mesenchymal cell derivatives. During embryonic development, cells become more specialized, and their early transcriptional plasticity and multilineage developmental potential is gradually restricted by epigenetic silencing of genes (19). 5-Azacytidine (AZA) is a nucleoside analog that is used to treat blood disorders such as myelodysplasia and leukemia (20). AZA demethylates DNA (21) and as an inducer of cell plasticity (22) is used in protocols to transdifferentiate cells in vitro (23–26) and to convert partially reprogrammed induced-pluripotent stem (iPS) cells to fully reprogrammed iPS cells (27). However, the capacity of AZA to induce cell plasticity has not to our knowledge been harnessed to generate tissue-regenerative multipotent stem (iMS) cells.

We hypothesized that AZA-induced cell plasticity occurs via a transient multi- or pluripotent cell state and that concomitent exposure to a receptive growth factor might result in the expansion of a plastic and proliferative population of cells. To this end, we treated lineage-committed cells with AZA and screened a number of different growth factors with known activity in mesenchyme-derived tissues and report that AZA in combination with platelet-derived growth factor–AB (PDGF-AB) converts primary somatic cells into iMS cells. Importantly, unlike primary MSCs (5), which may facilitate but do not directly contribute to tissue repair, iMS cells contribute directly to in vivo tissue regeneration in a context-dependent manner without forming teratomas.

Results

PDGF-AB/AZA-Induced Reversal of Lineage Commitment. To screen AZA/cytokine combinations for their potential to convert lineage-committed cells into proliferative multipotent stem cells, we first harvested bone marrow stromal cells from mice and differentiated them into osteocytes, chondrocytes, and adipocytes and used these in vitro-differentiated cells as a source (*SI Appendix*, Fig. S1). The quality of in vitro differentiation was assessed using immunohistochemistry, immunofluorescence, and transcriptomic analyses (*SI Appendix*, Fig. S2), and the cytokines [PDGFs, basic fibroblast growth factor (bFGF), hepatocyte growth factor (HGF), insulin-like growth factor (IGF), and vascular endothelial growth factor (VEGF)] were chosen for their known activity on mesenchyme-derived cells. In vitro-differentiated osteocytes, chondrocytes, and adipocytes were cultured in media for 12 d with or without cytokines. AZA was added to the cultures during the first 48 h, and a media-only control was always used (*SI Appendix*, Fig. S3*A*).

Osteocytes, chondrocytes, and adipocytes cultured in MSC medium supplemented with PDGF-AB and AZA demonstrated colony-forming potential that was comparable to that of primary bone marrow MSCs (bmMSCs) (*SI Appendix*, Fig. S3 *B* and *C*). By contrast, cells treated for a similar duration with either PDGF-AB or AZA alone or combinations of the other cytokines with or without AZA showed limited colony-forming unit-fibroblast (CFU-F) potential, and these colonies could not be replated (*SI Appendix*, Fig. S3 *C* and *Insets*). Notably, although primary bmMSCs and PDGF-AB and AZA-treated osteocyte (oCFU-Fs), chondrocyte (cCFU-Fs), and adipocyte (aCFU-Fs) cells could be serially passaged without reprogramming factors in the media, colonies generated from cells treated with PDGF-AB alone plateaued and failed to replate after a few passages (*SI Appendix*, Fig. S3*D*). Following PDGF-AB/AZA treatment, osteocytes, chondrocytes, and adipocytes also adopted gene expression profiles (*SI Appendix*, Fig. S4), cell surface markers (*SI Appendix*, Fig. S5), and differentiation characteristics (*SI Appendix*, Fig. S6) of primary undifferentiated bmMSCs. These screening experiments were repeated three times and also independently verified in a second laboratory (*SI Appendix*, Fig. S7).

Conversion of Primary Osteocytes from *Pdgfrα-H2B:GFP* Mice into Multipotent Proliferative MSC-Like Cells. To exclude the possibility that PDGF-AB/AZA-induced conversion was an artifact of residual bmMSCs in our in vitro differentiation assays, we evaluated the response of purified primary osteocytes to reprogramming [i.e., media + PDGF-AB/AZA (12/2 d)] or control media [i.e., media alone (12 d), media + PDGF-AB (12 d), or media + AZA (2 d)]. To this end, we harvested and treated Lin^-/$CD45^-$/$SCA1^-$/$CD31^-$/*Pdgfrα*-nuclear green fluorescence protein $(nGFP)^-$/$PDGFRA^-$/$CD51^+$ osteocytes (28) from long bones of *Pdgfrα-H2B:GFP* mice (29) (Fig. 1*A*). PDGFRA is expressed on cells with MSC activity (30), and we reasoned that conversion of osteocytes would be accompanied by expression of nGFP in previously nGFP-negative cells. Freshly harvested osteocytes from *Pdgfrα-H2B:GFP* mice were treated with PDGF-AB/AZA for 12 and 2 d, respectively (Fig. 1*B*). Primary osteocytes gained nGFP and lost CD51 expression when cultured in reprogramming media but not with control media (Fig. 1*C* and *SI Appendix*, Fig. S8*A*). Untreated osteocytes and osteocytes treated with AZA alone did not show any CFU-F activity (*SI Appendix*, Fig. S8*B*). On the other hand, osteocytes treated with PDGF-AB alone or PDGF-AB + AZA showed CFU-F activity, but long-term self-renewal was limited to osteocytes treated with both PDGF-AB and AZA (*SI Appendix*, Fig. S8 *B* and *C*). To record the conversion of treated osteocytes in real time, we also continuously live-imaged osteocytes harvested from *Pdgfrα-H2B:GFP* mice after the addition of reprogramming media (Movie S1). GFP-expressing cells were visible in reprogramming media as early as day 2, and their number increased progressively. This was accompanied by increased motility and cell division. Three biological repeats were performed. Cell cycle analysis showed that a higher proportion of PDGF-AB/AZA-treated osteocytes were in G2/M (*SI Appendix*, Fig. S8*D*).

The emergence of CFU-F activity was also evaluated from day 1 onwards and was noted to peak at approximately 8 d of supplementation with reprogramming media (Fig. 1*D*). The colony-forming potential in primary bmMSCs and treated osteocytes (oCFU-Fs) was predominantly within the *Pdgfrα*-nGFP–positive cell fraction (Fig. 1*E*). To interrogate qualitative differences between primary bmMSCs and reprogrammed osteocytes, micro-, small, and large colonies generated from GFP^+ stromal MSCs and osteocyte-derived oCFU-Fs were serially passaged to evaluate their growth potential (Fig. 1*F*). Micro colonies from primary bmMSCs could not be serially passaged, and small colonies waned after a few passages. Continuous culture was possible only for the large colonies. In contrast, irrespective of size, all colonies generated by oCFU-Fs at the first passage had the intrinsic capacity to self-renew. This suggested that within micro- and small colonies generated from oCFU-F resided cells that had not yet gained their full potential. To systematically evaluate this, we performed serial replating of single cells from individual colonies (*SI Appendix*, Fig. S9). Micro colonies generated by primary bmMSCs could not be propagated, whereas cells within large colonies retained their heterogeneous colony-forming potential through serial passages (*SI Appendix*, Fig. S9, *Left*). In contrast, first- and second-generation micro colonies generated by oCFU-Fs

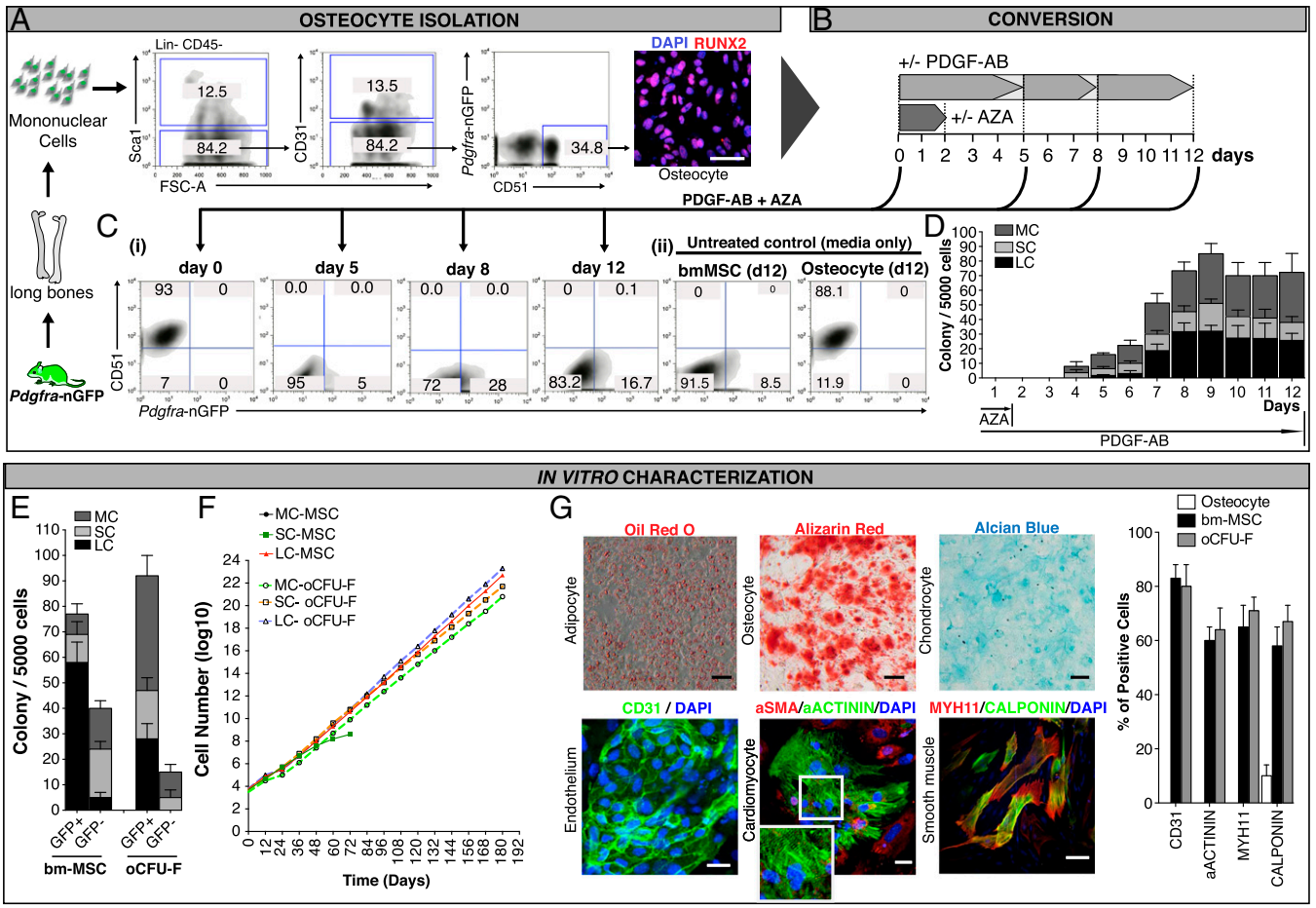

Fig. 1. Conversion of primary osteocytes from *Pdgfrα-H2B:GFP* mice into renewable multipotent cells. (*A*) Sorting strategy for harvesting Lin$^-$/CD45$^-$/SCA1$^-$/CD31$^-$/*Pdgfrα*-GFP$^-$/CD51$^+$ osteocytes from long bones of 8–16-wk-old mice. The *Inset* shows expression of RUNX2 by confocal immunofluorescence in sorted osteocytes. (*B*) Schematic outline of the treatment schedule. Osteocytes from *A* were treated and evaluated by flow cytometry (*C*) and CFU-F assays (*D*). (*C*, *i*) Flow cytometry profiles of freshly isolated *Pdgfrα*-GFP$^-$/CD51$^+$ osteocytes showing progressive loss of CD51 and acquisition of GFP when cultured in media containing PDGF-AB and AZA. (*ii*) Primary osteocytes treated with media alone did not show acquisition of GFP. A proportion of primary MSCs harvested from bone continue to express GFP. (*D*) Quantification of oCFU-F colonies (based on size) from osteocytes cultured in MSC medium supplemented for 1–12 and 1–2 d with PDGF-AB and AZA, respectively. (*E*) CFU-F colony number (based on size) derived from sorted bmMSCs and sorted oCFU-Fs. (*F*) Growth curves of micro-, small, and large colonies from bmMSCs and oCFU-Fs that were harvested at P1 and perpetuated in culture. (*G*) Histo- and immunohistochemistry showing multilineage differentiation potential of converted oCFU-Fs. The histogram to the *Right* shows a comparison of differentiation markers (see *Lower* panel of images) in untreated osteocytes, bmMSCs, and oCFU-Fs. Also see *SI Appendix*, Fig. S10 for an extended panel of tissue differentiation markers and quantification. bmMSCs, primary bone marrow mesenchymal stem cells; oCFU-F, colony-forming unit–fibroblasts derived from PDGF-AB/AZA-treated osteocytes. CFU-Fs were scored as micro- (MC, 5–24 cells, <2 mM), small (SC, ≥25 cells, 2–4 mM), or large (LC, >4 mM) colonies (46). (Scale bar, 20 μm.) SD bars, SD between three independent experiments.

formed colonies that could propagate, but with serial passages, this capacity was lost (*SI Appendix*, Fig. S9, *Right*).

To evaluate their differentiation potential, we first induced oCFU-Fs generated from primary osteocytes into bone, cartilage, and fat (Fig. 1*G*). oCFU-Fs also demonstrated in vitro differentiation potential into different mesodermal [endothelium (VE-Cad, CD31, CAV1, vWF, eNOS, ac-LDL uptake), muscle (aSMA, MYH11, MYOCD, SRF), cardiomyocyte (NKX2.5, MEF2C, CX43, GATA4, contractility), neuroectodermal (neural; Tuj1, GFAP, O4)] and endodermal lineages (hepatocyte; Albumin, HNF-4a) with comparable efficiency to primary bmMSCs (Fig. 1*G* and *SI Appendix*, Fig. S10). In some respects, the potency of oCFU-Fs exceeded that of bmMSCs. Cardiomyocytes generated from oCFU-Fs but not bmMSCs showed spontaneous rhythmic contractility of ∼4.5 beats per second (Movie S2), and endothelial tubes generated in matrigel from oCFU-Fs but not bmMSCs showed PDGFRB$^+$ pericytes enveloping CD31$^+$ endothelial cells (*SI Appendix*, Fig. S10*B* and Movie S3). Neither bmMSCs nor oCFU-Fs formed teratomas when transplanted under the kidney capsule and cannot be considered pluripotent by this criterion. Although lacking intrinsic teratoma potential, oCFU-Fs (ubiquitously expressing cytoplasmic GFP) when cotransplanted with ESCs contributed to a range of mesodermal, neuroectodermal, and endodermal lineages (*SI Appendix*, Fig. S11). These data show that oCFU-Fs have intrinsic plasticity and can be induced to differentiate into multiple tissue types in vivo in response to regional cues (in this instance supplied by ESCs) (*SI Appendix*, Fig. S11). Notably, although bmMSCs show comparable in vitro plasticity, when cotransplanted with ESCs, they did not contribute to cells within teratomas. These data reiterate the limited in vivo plasticity of primary MSCs.

To evaluate the robustness of PDGF-AB/AZA in converting primary cells, we also harvested Lin$^-$/CD45$^-$/SCA1$^-$/CD31$^-$/PDGFRA$^-$/CD51$^+$ osteocytes from different mouse strains. Quantitative differences were observed between mouse strains, with C57BL6 and Q-Swiss strains showing higher oCFU-F activity (after 12 d of treatment) than those derived from Rag1 (B6.SVJ129-Rag1^{tm1Bal}) mice (*SI Appendix*, Fig. S12), but conversion was achieved in all.

Conversion of Primary Subcutaneous Adipocytes from *Pdgfrα-H2B:GFP* Mice into MSC-Like Cells. To establish that PDGF-AB/AZA-mediated conversion was not limited to primary osteocytes, we harvested subcutaneous (s.c.) fat from *Pdgfrα-H2B:GFP* mice and treated primary mature adipocytes with reprogramming or control media and functionally analyzed the treated cells (*SI Appendix*, Fig. S13*A*). Primary mature adipocytes (*SI Appendix*, Fig. S13*B*) were also continuously live imaged to trace cell conversion. A proportion of harvested mature adipocytes in reprogramming media gained PDGFRA (nGFP) expression as early as day 2, and their number increased during the 8-d period of live imaging (Movie S4). *Pdgfra*-nGFP expression in PDGF-AB/AZA-treated adipocytes (aCFU-Fs) at day 12 was comparable to primary adipocyte-derived MSCs harvested from *Pdgfrα-H2B:GFP* mice (*SI Appendix*, Fig. S13*C*). The colony-forming potential in primary adipocyte-derived MSCs and in aCFU-Fs resided predominantly within the *Pdgfra*-nGFP–positive cell fraction (*SI Appendix*, Fig. S13*D*), and both adipocyte-derived MSCs and aCFU-Fs showed robust trilineage differentiation potential (*SI Appendix*, Fig. S13*E*) in three biological replicates.

Conversion of Primary Human Mature Adipocytes into MSC-Like Cells. To investigate whether primary human adipocytes were also amenable to conversion, we harvested s.c. fat and treated mature adipocytes (*SI Appendix*, Fig. S14*A*) with reprogramming (PDGF-AB + AZA) or control media (PDGF-AB or AZA or media alone) substituting recombinant murine with recombinant human PDGF-AB. By day 25, a proportion of adipoctyes treated with reprogramming media lost their fat globules and adopted stromal cell morphology (*SI Appendix*, Fig. S14*B*). Adipocytes treated with reprogramming but not control media also demonstrated large colony CFU-F potential, albeit lower than that of primary human adipose-derived stromal cells (*SI Appendix*, Fig. S14*C*), long-term growth (*SI Appendix*, Fig. S14*D*), and trilineage differentiation potential (*SI Appendix*, Fig. S14*E*).

Contribution of PDGF-AB/AZA-Treated Primary *Dmp1*-eYFP+ Osteocytes to in Vivo Tissue Regeneration. To evaluate contributions from treated osteocytes to in vivo tissue regeneration, we required a trackable marker that would be retained in cell progeny derived from osteocytes. Dentin matrix acid phosphoprotein 1 (DMP1) marks terminally differentiated osteocytes (31). We crossed *Dmp1*-cre transgenic mice with *R26R*-eYFP mice to generate transgenics with eYFP-labeled osteocytes that could be treated with PDGF-AB/AZA and traced in vivo. Consistent with their osteocytic identity, SCA1$^-$/CD31$^-$/PDGFRA$^-$/*Dmp1*eYFP$^+$ cells coexpressed CD51 (*SI Appendix*, Fig. S15*A*) and displayed the characteristic morphology of mature osteocytes (Fig. 2*A*). These cells were sorted and cultured with or without PDGF-AB and/or AZA (Fig. 2 *A* and *B*) and evaluated by flow cytometry and CFU-F assays at day 12 (Fig. 2 *C* and *D*) and by in vivo transplantation assays (Fig. 2 *E* and *F*). The morphology of osteocytes changed from cells with a globular soma and fine-branching cytoplasmic extensions to flat elongated stromal cells (Fig. 2*A*). In contrast to untreated cells, PDGF-AB and AZA-treated *Dmp1*eYFP$^+$ osteocytes acquired MSC markers at day 12, albeit at

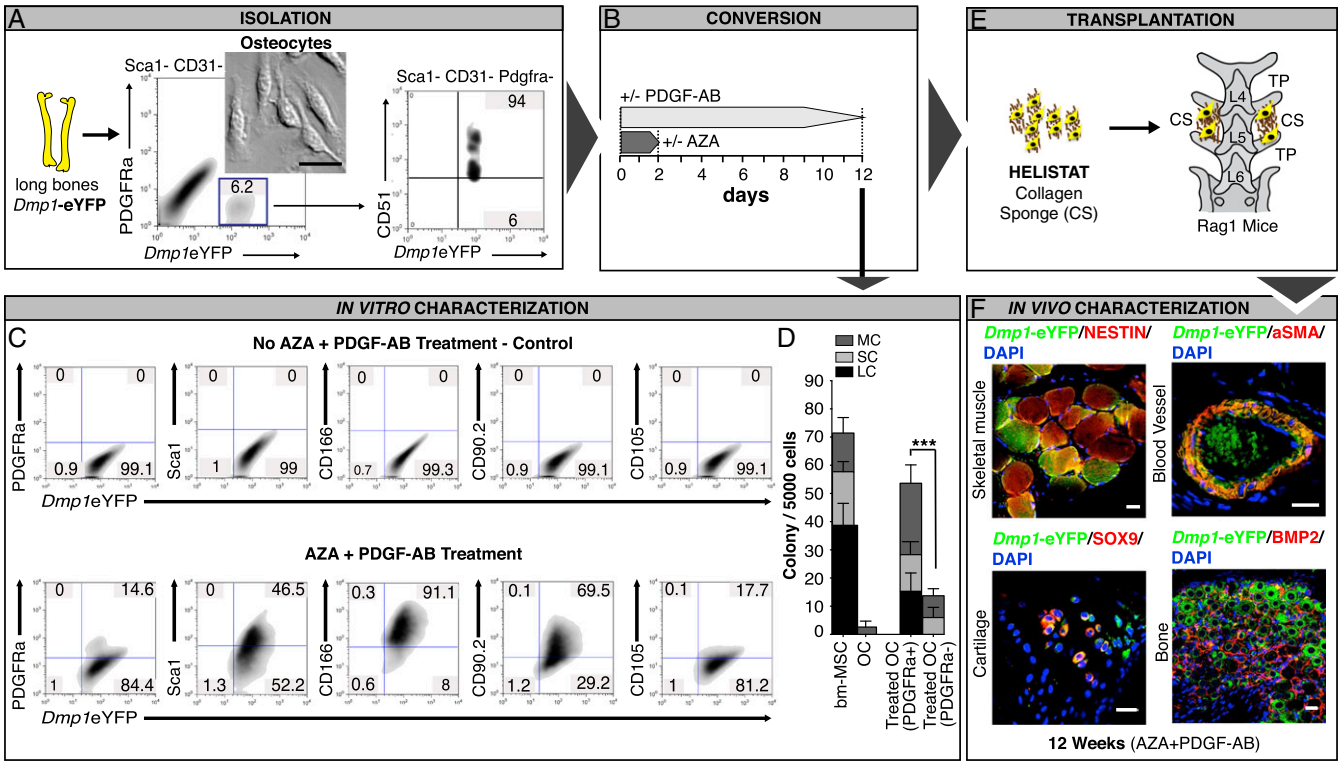

Fig. 2. PDGF-AB/AZA-treated *Dmp1*-eYFP osteocytes acquire MSC markers and CFU-F activity and show in vivo multipotency in a tissue injury model. (*A*) Isolation of osteocytes from *Dmp1*-eYFP mice. *Dmp1*-eYFP+ cells also express the osteocyte marker CD51 and show morphology characteristic of osteocytes. (*B*) Schematic outline of the treatment options applied to osteocytes from *A*. (*C*) Flow cytometry analysis showing the acquisition of MSC markers on primary *Dmp*1-eYFP$^+$ osteocytes maintained in media for 12 d with (*Lower*) and without (*Upper*) PDGF-AB/AZA. (*D*) Number and size distribution of plastic adherent CFU-F colonies. (*E*) Schematic representation of the posterior–lateral intertransverse lumber fusion model used for the implantation of Helistat collagen sponges containing PDGF-AB/AZA-treated or control (PDGF-AB alone, AZA alone, or no PDGF-AB or AZA) *Dmp1*eYFP$^+$ osteocytes. (*F*) Confocal images of transplanted tissues harvested at 12 wk from a mouse engrafted with PDGF-AB/AZA-treated *Dmp1*eYFP cells showing the donor cell contribution to regenerating skeletal muscle, blood vessels, bone, and cartilage. Also see *SI Appendix*, Fig. S15 for controls and in vivo reexpression of stroma cell markers in *Dmp1*-eYFP cells. (Scale bar, 20 μm.) SD bars, SD between three independent experiments. bmMSCs, primary bone marrow mesenchymal stem cells; CS, collagen sponge; *Dmp1*, dentin matrix acid phosphoprotein 1; oCFU-F, colony-forming unit–fibroblasts derived from PDGF-AB/AZA-treated osteocytes; TP, transverse process.

varying frequency (Fig. 2*C*). A fraction of *Dmp1*eYFP$^+$ osteocytes (~15%) treated with PDGF-AB/AZA acquired PDGFRA (Fig. 2*C*). The PDGFRA +ve and –ve fractions were sorted and their CFU-F activity assessed and compared with that of primary bmMSCs and untreated osteocytes (Fig. 2*D*). Whereas untreated osteocytes could not form CFU-Fs, treated osteocytes that acquired surface PDGFRA acquired CFU-F potential. This experiment was repeated twice.

To establish whether PDGF-AB/AZA-treated osteocytes contributed to tissue regeneration, cells were then loaded into Helistat collagen sponges and transplanted into the postero-lateral gutters adjacent to decorticated lumbar vertebrae (Fig. 2*E*) (32). Tissue sections were harvested at 12 wk posttransplantation and subjected to analysis (Fig. 2*F*). The surgeon (W.W.) and the scientist performing the histological analysis (R.A.O.) were blinded to the treatment groups. Reprogrammed *Dmp1*eYFP$^+$ oCFU-Fs expressed MSC markers such as PDGFRA and Vimentin (*SI Appendix*, Fig. S15*D*) and contributed to new skeletal muscle (Nestin), blood-filled vessels (aSma), and cells of bone (BMP2) and cartilage (SOX9) lineages (Fig. 2*F*). In contrast to oCFU-Fs, untreated SCA1$^-$/CD31$^-$/PDGFRA$^-$/*Dmp1*eYFP$^+$ osteocytes and primary bmMSCs (derived from *b2-microglobulin*-GFP mice to track their tissue contribution) did not show evidence of in vivo proliferation or transdifferentiation.

We also evaluated the potential for PDGF-AB and AZA-treated allogeneic bone fragments to fuse with decorticated vertebrae in the lumbar spinal fusion mouse model used above. Long bones were harvested from ubiquitous GFP mice (*β2 microglobulin*-GFP) (33), flushed to evacuate bone marrow, fragmented, and collagenase-treated to denude surface-adherent cells (Fig. 3*A*). The bone fragments were cultured in MSC medium alone or supplemented with PDGF-AB and/or AZA for 12 d before transplantation (Fig. 3 *B* and *C*). Again, the surgeon (W.W.) and the scientist performing the histological analysis (R.A.O.) were blinded to the treatment groups. Bone fragments treated with PDGF-AB and AZA but not untreated fragments or fragments treated with either PDGF-AB or AZA alone showed radiographic evidence of de novo activity both at 6 and 12 wk (Fig. 3*D*). Histological sections of tissues harvested from graft sites at 6 and 12 wk showed new woven bone with marrow-filled spaces and cartilage adjacent to transplanted fragments (Fig. 3 *E*, *i* and *ii*). Immunohistochemistry of retrieved tissues showed that PDGF-AB + AZA-treated bone fragments but not untreated or bone fragments treated with PDGF-AB or AZA alone showed a rim of GFP$^+$ cells, with some coexpressing the transient myoblast marker α-smooth muscle actin (aSMA) and stromal cell markers PDGFRA, CD166, and Vimentin extruding into the surrounding matrix (*SI Appendix*, Fig. S16*A*). Cells of bone (BMP2, RUNX2), cartilage (SOX9), skeletal muscle (Nestin, Desmin, M-Cadherin), blood vessels (aSMA, CD146$^+$ pericytes, and VE-Cadherin$^+$ endothelial cells), blood, and blood derivatives (Cathepsin-K osteoclasts) were readily identified adjacent to and were derived from

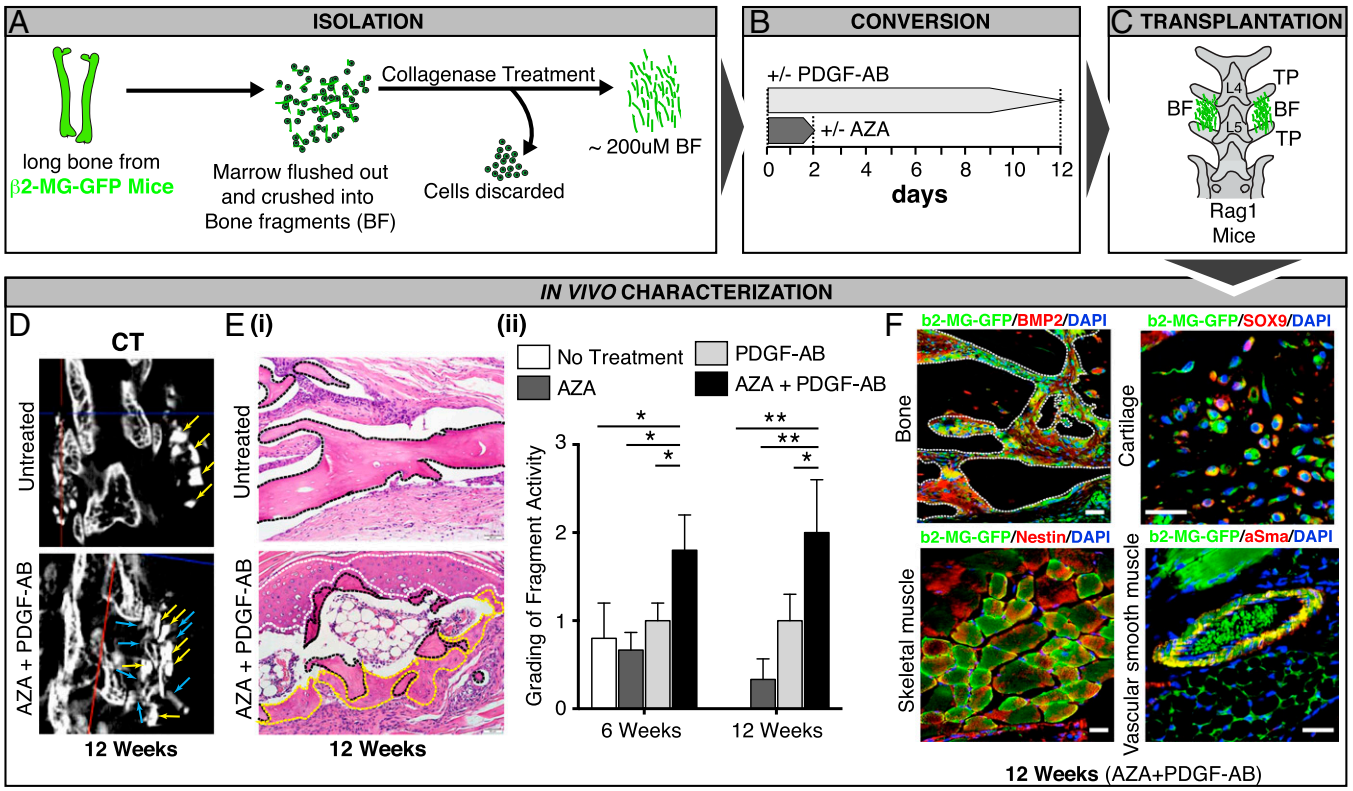

Fig. 3. PDGF-AB/AZA-treated bone fragments contribute to tissue repair and regeneration. (*A*) A schematic representation of the experimental steps involved in harvesting bone and producing fragments stripped of bone-associated stromal cells from a ubiquitous GFP (*β2microglobulin*-GFP) mouse. (*B*) Schematic outline of the treatment options applied to bone fragments from *A*. (*C*) Schematic of the posterior–lateral intertransverse lumber fusion model used to engraft treated and control bone fragments from *B*. (*D*) Micro-CT images of mice implanted with untreated and PDGF-AB/AZA-treated bone fragments at 12 wk. Yellow arrows show allograft material, and blue arrows show de novo activity of treated bone fragments. (*E*, *i*) Hematoxylin and eosin-stained sections of implanted fragments and surrounding tissues harvested at 6 and 12 wk. Untreated bone fragments (black dot lines) (*Top*) showed no new bone generation, whereas treated bone fragments (black dot lines) (*Bottom*) show new woven bone (yellow dot lines) with cartilage (white dot lines) and marrow. (*ii*) Graph showing graded response of PDGF-AB/AZA-treated and control bone fragments at 6 and 12 wk. (*F*) Confocal images of tissues surrounding treated bone fragments showing donor cell contribution to bone, cartilage, skeletal muscle, and blood vessels. Also see *SI Appendix*, Fig. S16 for an extended panel of stromal and tissue differentiation markers on donor-derived cells in vivo. (Scale bar, 20 μm.) SD bars, SD between independent experiments. *$P < 0.05$ and **$P < 0.01$ (Student's *t* test). BF, bone fragment; TP, transverse process.

transplanted PDGF-AB/AZA-treated GFP$^+$ bone fragments at 6 and 12 wk (Fig. 3*F* and *SI Appendix*, Fig. S16*B*).

Given the potential clinical significance of these observations, we specifically surveyed both 6- and 12-wk grafts from both osteocyte and bone fragment transplants for any evidence of teratoma formation and report that there were none. There was also no difference in G-banded mouse karyotypes following PDGF-AB/AZA treatment. The perceived benefits of MSC transplants have been attributed to their immunomodulatory properties. To evaluate the immunomodulatory properties of oCFU-Fs, we performed mixed lymphocyte reaction (34) assays. Both control bmMSCs and oCFU-Fs were capable of suppressing T-cell proliferation, with the latter showing more pronounced effects (*SI Appendix*, Fig. S17 *A*, *i* and *ii*). T-cell production of Granzyme B, an effector molecule, was also suppressed by both bmMSCs and oCFU-Fs but not control primary osteocytes (*SI Appendix*, Fig. S17*B*). This experiment was repeated twice.

Signaling Through PDGFRA Is Required for Cell Conversion. PDGF-AA and PDGF-BB homodimers could not be substituted for PDGF-AB heterodimers. Although both PDGF-AA ± AZA and PDGF-BB ± AZA-treated osteocytes generated primary CFU-F colonies (*SI Appendix*, Fig. S18 *A*, *i* and *ii*), the former could only be cultured for a limited number of passages and the latter could not be passaged at all (*SI Appendix*, Fig. S18*B*). To dissect signaling events associated with cell conversion, we isolated primary osteocytes from long bones and evaluated the acquisition of CFU-F activity in the presence of inhibitors that target various components of PDGFR signaling (Fig. 4 *A*–*C*). Intracelullar signaling downstream of the PDGF receptor complex is multifactorial. To guide our choice of inhibitors, we took advantage of Ingenuity pathway analysis comparing expression levels of various mediators of PDGFR signaling between pre– and post–PDGF-AB/AZA-treated osteocytes, which showed activation of components of the JAK/STAT and JNK/c-JUN but not PI3Kinase pathways in the latter (*SI Appendix*, Fig. S19). pSTAT3, pJNK1, and pcJUN protein levels were significantly elevated in osteocytes 48 h after treatment with PDGF-AB and AZA, and these increases were modulated by their respective inhibitors (Fig. 4*D*).

PDGF-AB binds PDGFR αα-receptor homodimers and αβ-receptor heterodimers (20). Inhibition of PDGF receptor signaling using a nonselective inhibitor, AG1296, or APA5, a selective monoclonal PDGFRA inhibitor, abolished PDGF-AB/AZA–mediated oCFU-F production from primary osteocytes (Fig. 4 *E*, *i* and *ii*). Interestingly, primary osteocytes express PDGFRB but not PDGFRA (*SI Appendix*, Fig. S20*A*). However, within 48 h of PDGF-AB/AZA treatment, surface PDGFRA was induced in a fraction (~6%) of osteocytes. AZA alone or PDGF-AB alone also induced PDGFRA expression, albeit to a lesser extent (*SI Appendix*, Fig. S20*B*). There was a dose-dependent decrease in oCFU-F production when osteocytes were converted in the presence of JAK/STAT3 and JNK inhibitors (Fig. 4 *E*, *iii*–*v*). The combination of STAT3 and JNK inhibitors was even more effective than either alone (Fig. 4 *E*, *vi*) but did not completely abolish large colony formation at the concentrations used. PI3kinase pathway inhibitors Wortmannin and LY294002, on the other hand, had no impact on oCFU-F production (Fig. 4 *E*, *vii*).

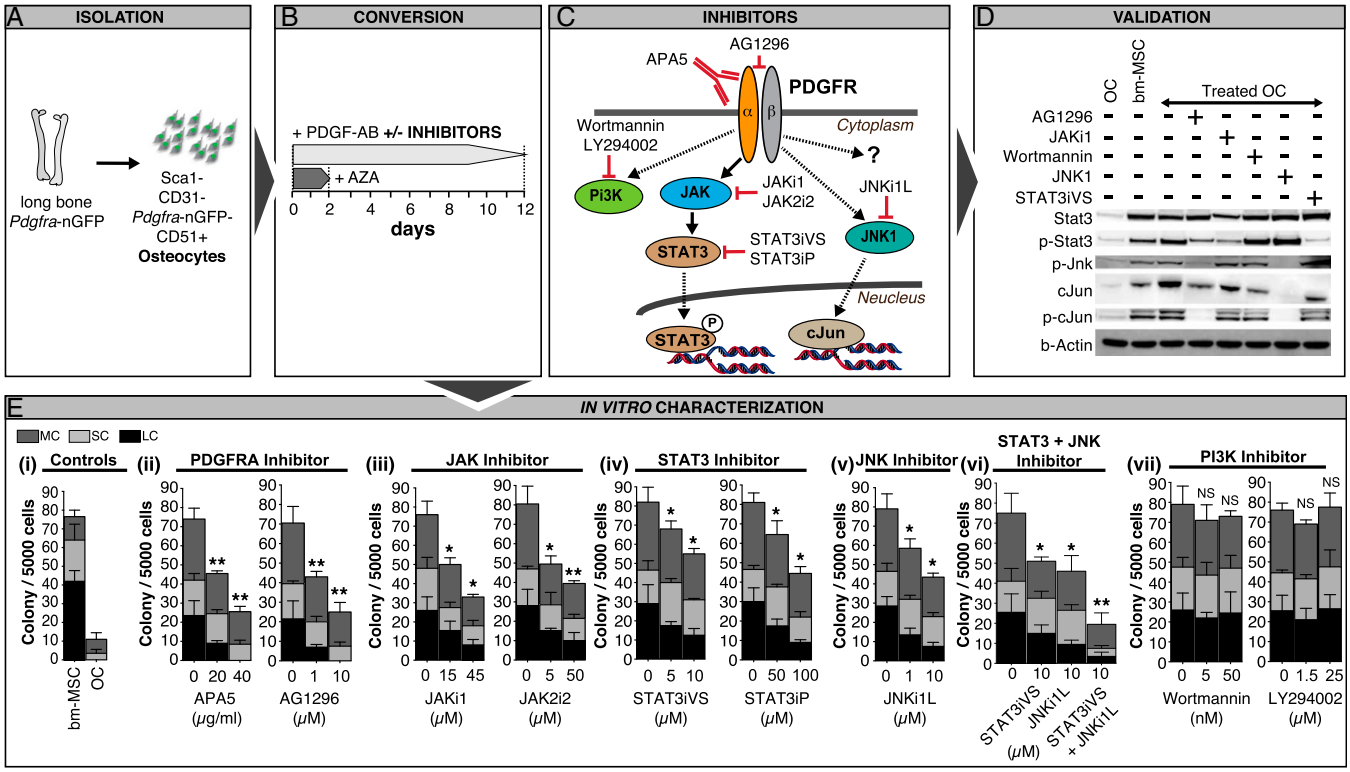

Fig. 4. Signaling through PDGFRA is required for cell conversion. (*A*) Schematic diagram of primary osteocytes harvested by FACS from *Pdgfrα-H2B:GFP* mice. (*B*) Schematic outline of PDGF-AB/AZA treatment of osteocytes (from *A*) with/without inhibitors. (*C*) Schematic diagram of PDGFRA signaling and choice of targets for inhibition. (*D*) Western blots performed at 48 h of treatment (see *B*). (*E*) Colony-forming capacity of (*i*) bmMSCs, osteocytes, and PDGF-AB/AZA-treated osteocytes with inhibitors of (*ii*) PDGFRA (APA5) and PDGFRA/PDGFRB (AG1296), (*iii*) JAK (JAK2i2 and JAKi1) and (*iv*) STAT3 (STAT3iVS and STAT3iP) signaling, (*v*) Jnk/cJUN (JNKi1L; a Jnk inhibitor) and (*vi*) dual inhibition of STAT3 and JNK signaling, and (*vii*) PI3K (Wortmannin and LY294002) signaling. bmMSCs, primary bone marrow mesenchymal stem cells; OC, osteocytes. SD bars, SD between independent experiments. *$P < 0.05$ (Student's *t* test). CFU-Fs scored as micro- (MC, 5–24 cells, <2 mM), small (SC, ≥25 cells, 2–4 mM), or large (LC, >4 mM) colonies.

PDGF-AB/AZA-Treated Osteocytes Reexpress Pluripotency Factors and Have a Distinct Transcriptional Profile. The global gene expression profiles of primary osteocytes treated with PDGF-AB/AZA place these cells closer to MSCs than to any other tissue-specific or pluripotent stem cells (Fig. 5*A*). However, their profiles do not overlap. Nucleosome occupancy and DNA methylation at gene promoters are two early and late events, respectively, that are associated with gene silencing that we predicted would change during cell conversion as previously silenced genes are reexpressed (35, 36). To this end, we used nucleosome occupancy and methylome sequencing (NOMe-Seq) and allelic bisulphite sequencing to assess nucleosome occupancy and DNA methylation, respectively, at promoters of lineage commitment and pluripotency genes. *Runx2* expression is associated with

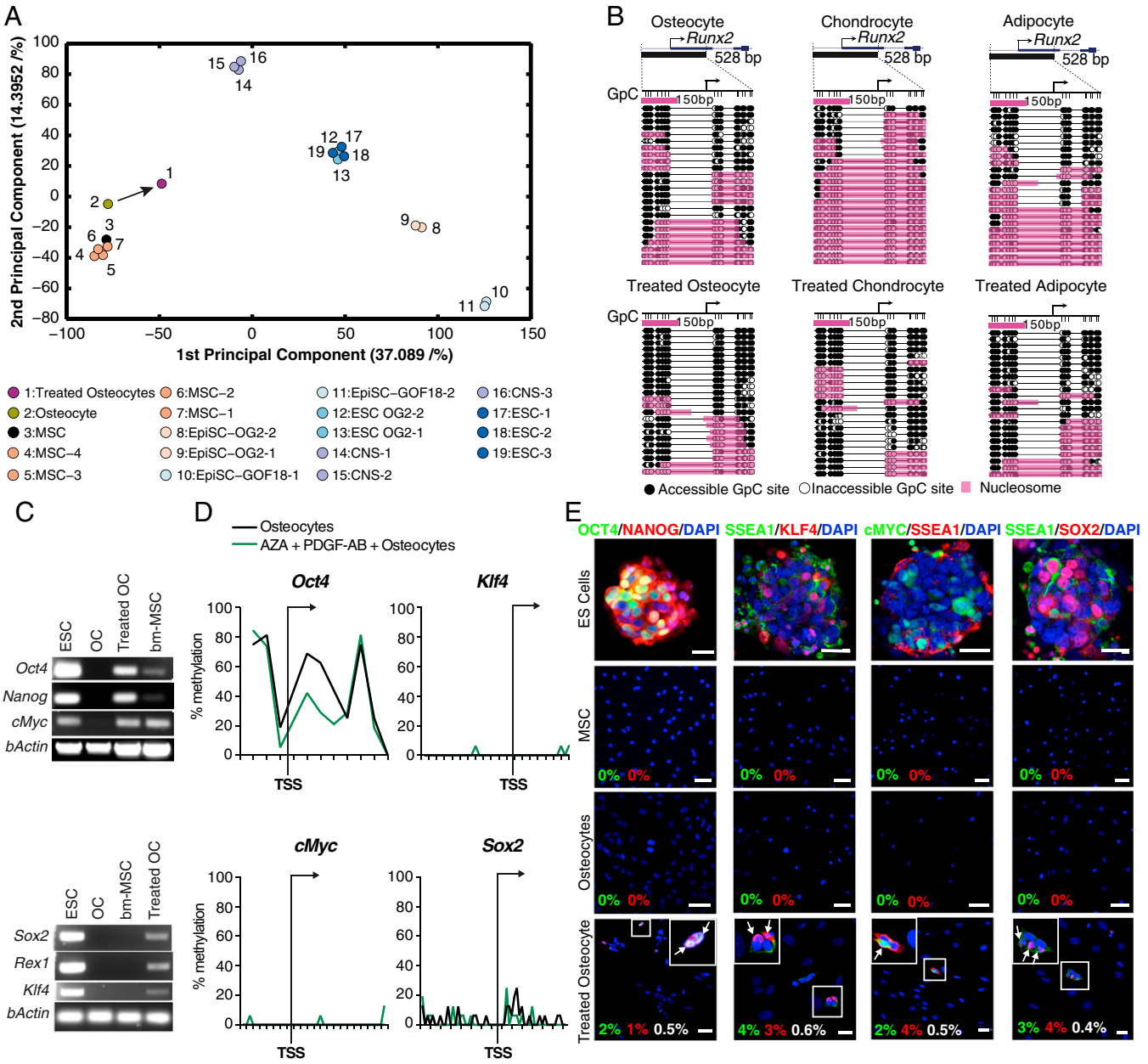

Fig. 5. PDGF-AB/AZA-treated osteocytes reexpress pluripotency factors and have a distinct transcriptional profile. (*A*) A principal component analysis of the transcriptomes of primary osteocytes and PDGF-AB/AZA-treated osteocytes relative to mESCs, mEpiblast stem cells, primary MSCs, and neural stem cells. (*B*) NOMe-Seq analysis of *Runx2* promoter accessibility in osteocytes, chondrocytes, and adipocytes is shown (*Top*). (*Bottom*) PDGF-AB/AZA-treated counterparts of osteocyte, chondrocyte, and adipocyte. NOMe-Seq uses a DNA methyltransferase that methylates DNA at GpC sites. DNA methylation (artificially introduced by the GpC methylase at GpC sites or endogenous methylation at CpG sites) is determined by bisulphite sequencing. GpC sites are represented as circles and are shaded black when accessible and white when inaccessible to the DNA methylase. Contiguous sites of DNA inaccessibility of ~150 bp indicate sites occupied by nucleosomes (pink bars). Sequencing results for 24 individual alleles are shown for each cell type. (*C*) RT-PCR expression of pluripotency genes in primary osteocytes, primary bmMSCs, PDGF-AB/AZA-treated osteocytes, and mESCs. (*D*) Fraction of methylated CpGs at the promoters of *Oct4*, *Klf4*, *cMyc*, and *Sox2* (see *SI Appendix*, Fig. S21 for bisulfite sequencing results of individual alleles). (*E*) Confocal images of immunohistochemical stains of ESCs, bmMSCs, primary osteocytes, and PDGF-AB/AZA-treated osteocytes showing OCT4/Nanog, KLF4/SSEA1, cMYC/SSEA1, and SOX2/SSEA1 expression. Dual staining in PDGF-AB/AZA-treated osteocytes is shown by white arrows, and the percentages of cells expressing single/double stains are listed. (Scale bar, 20 μm.)

commitment to the osteogenic lineage (37) and is transcribed from a promoter that is devoid of CpGs. *Runx*2 promoter alleles were mostly free of nucleosomes in osteocytes and adipocytes but nucleosome-dense in chondrocytes (Fig. 5*B*, *Upper*). PDGF-AB/AZA treatment evicted nucleosomes from the *Runx*2 promoter in all cell types (Fig. 5*B*, *Lower*).

PDGF-AB/AZA-treated osteocytes expressed pluripotency genes *Oct4*, *cMyc*, *Nanog*, *Klf4*, *Sox2*, and *Rex1*, but their levels were substantially lower than in ES cells (Fig. 5*C*). Primary osteocytes did not express any of these genes, whereas primary early passage bmMSCs, although not expressing *Klf4*, *Sox2*, or *Rex1*, did express *cMyc* at levels that were equivalent to, and *Oct4* and *Nanog* levels that were less than, those in PDGF-AB/AZA-treated osteocytes. Given the reexpression of pluripotency genes in lineage-committed cells following PDGF-AB/AZA treatment, we performed bisulphite sequencing on primary osteocytes before and after PDGF-AB/AZA treatment to assess DNA methylation profiles at the promoters of *Oct*4, *Sox*2, *Klf*4, and *c-Myc* (Fig. 5*D* and *SI Appendix*, Fig. S21 *A–D*). The majority of *Oct*4 alleles in osteocytes showed CpG methylation at their transcription start sites (TSSs). There was significant reduction of methylation at the *Oct4* TSS following PDGF-AB/AZA treatment. Interestingly, almost none of the *Sox*2, *Klf*4, and *c-Myc* alleles even in pretreatment osteocytes had methylation of CpGs at their TSSs (Fig. 5*D*). The corresponding proteins were detectable by immunohistochemistry in 1–4% of treated osteocytes but not in pretreatment osteocytes or MSCs (Fig. 5*E*). It is noteworthy that nuclear staining of these transcription factors in treated osteocytes is sparse in contrast with the diffuse staining seen in ESCs where these factors are abundant (Fig. 5*E* and *SI Appendix*, Fig. S21*E*). There is also heterogeneity of expression of pluripotent factors within a single converted osteocyte. The heterogeneity and infrequency of expression of these proteins was consistent with primary CFU-F activity (~1% of plated cells) observed in treated osteocytes (Fig. 1*D*). Taken together, these data show that PDGF-AB/AZA treatment converts primary lineage-committed cells into cells that have features of MSCs but possess greater in vitro differentiation capacity and in vivo plasticity and are distinct from pluripotent cells in their inability to form spontaneous teratomas and low expression of pluripotent factors and hence were termed iMS cells.

Discussion

iMS cells share a number of in vitro features with tissue-derived MSCs. However, iMS cells are transcriptionally distinct and have major in vivo advantages over MSCs, including their cellular plasticity, retention at graft sites, and contribution to tissue regeneration (*SI Appendix*, Table S1). The conversion process requires culturing cells or tissues transiently with AZA and PDGF-AB. AZA is administered to patients with myelodysplasia as a daily injection for 7 consecutive days (or interrupted by the weekend) followed by 3 wk off treatment (20). This 28-d cycle is repeated for as long as patients show benefit and often continues for many years. The dose of AZA (10 μM) that was required in conjunction with PDGF-AB to generate iMS cells was selected after testing concentrations within the peak plasma concentrations measured in patients (38, 39). AZA is incorporated into DNA and RNA (38), and PDGF-AB is both a mitogen and cell survival factor (40–42). If PDGF-AB stimulation contributes to the uptake of AZA and proliferation of an otherwise transient cell population, it is unclear at this stage why PDGF-AB succeeds when the other cytokines do not. It is noteworthy that the endogenous expression patterns of PDGF-A and PDGF-B do not frequently overlap (40) and PDGF-AB heterodimers may be infrequent in vivo.

It is possible that the early effect of AZA is to facilitate reexpression of genes that are required for cell conversion. For example, primary osteocytes lack PDGFRA expression, but as shown in Fig. 4*E*, PDGFRA-mediated signaling is required for cell conversion. Surface PDGFRA protein expression is induced by AZA and further enhanced by PDGF-AB, which requires PDGFRA for canonical signaling (*SI Appendix*, Fig. S20). Oct4 reexpression appears to be a key step in the evolution of somatic cells toward pluripotency (43). The exact sequence of events that leads to demethylation of the *Oct4* promoter and *Oct4* reexpression as well as nucleosome eviction at lineage-specific gene promoters following PDGF-AB/AZA treatment will require further investigation. Given the transcriptional connectivity of pluripotent genes (44), *Oct4* reexpression in osteocytes by promoter demethylation may serve as the driver for reexpression of the others. The erasure of epigenetic barriers at lineage-committed genes is probably as important as the reactivation and low-level reexpression of pluripotent genes for the plasticity of these reprogrammed cells.

The combination of PDGF-AB and AZA is also effective in converting primary human adipocytes in serum-free medium into proliferative CFU-Fs that can be extensively passaged in vitro (*SI Appendix*, Fig. S14). For both murine and human cells, further research is required to establish how transplanted iMS cells activate lineage-specific transcriptional programs in response to local cues and the range of tissues that can be generated in vivo. It will also be important to determine whether and for how long undifferentiated iMS cells remain dormant at sites of transplantation and retain their capacity to proliferate and differentiate on demand. Although there was no evidence of systemic spread or tumourigenicity at 12 wk, long-term evaluation will be necessary before clinical application. Nevertheless, this efficient vector-free method of generating autologous tissue-regenerative cells has significant merits over current approaches.

Materials and Methods

Mice. All experiments involving mice were approved by the University of New South Wales animal ethics committee. The strains are detailed in *SI Appendix*.

BmCFU-F Isolation and ex Vivo Expansion. BmCFU-Fs were isolated from wild-type C57BL/6, Q(S), Rag1, Pdgfrα-nGFP, or DMP1eYFP mice. Tibias and femurs were removed, cleaned of excess soft tissues, flushed out and thoroughly crushed using a mortar and pestle, and collagenase-treated, and the filtered supernatant was inactivated and plated in αMEM with 20% (vol/vol) FCS and penicillin/streptomycin/glutamine (P/S/G) (see *SI Appendix*).

Primary Osteocyte Isolation and Culture. Osteocytes were isolated from long bones of 8–16-wk-old wild-type C57BL/6, Q(S), Rag1, or Pdgfrα-nGFP mice. Cells were FACS sorted for $SCA1^{-}/CD31^{-}/PDGFRA^{-}/CD51^{+}$ and cultured in DMEM + P/S/G + 100 μg/mL of ascorbate + 10% FCS (see *SI Appendix*).

Primary Mature s.c. Adipocyte Isolation and Culture. Primary mature s.c. adipocytes were isolated from 8- to 16-wk-old PDGFRA-nGFP mice adipose tissue using a previously described method (45). Primary adipocytes were cultured in adipocyte medium (DMEM-HG + 10% FCS + P/S/G) at 37 °C and 5% CO_2 in the incubator for 8–10 d before exposing to reprogramming agents (see *SI Appendix*).

Primary Osteocyte Isolation and Culture from DMP1-eYFP Mice. Primary osteocytes were isolated from long bones of 8–16-wk-old DMP1-eYFP mice. Cell suspensions from the primary isolation procedure and resulting bone fragments were cultured on type-I rat tail collagen-coated six-well plates in αMEM + 5% FCS + P/S/G for 7 d. Outgrowths of cells from bone fragments and cells in suspension were FACS-sorted for $SCA1^{-}/CD31^{-}/PDGFRA^{-}/DMP1eYFP^{+}$ and cultured in osteocyte culture media for 3 d before replacement with reprogramming medium (see *SI Appendix*).

Cellular Reprogramming.

Reprogramming in vitro-generated mouse osteocytes, chondrocytes, and adipocytes. In vitro-differentiated osteocytes, chondrocytes, and adipocytes were first cultured in MSC medium (αMEM + 20% FCS + P/S/G) with or without 10 μM AZA (Tocris Biosciences) and with or without cytokine (50 or 100 ng/mL Pdgf-AA or Pdgf-BB or Pdgf-AB, 10 ng/mL basic fibroblast growth factor, 20 ng/mL hepatocyte growth factor, 10 ng/mL insulin-like growth factor, and 10 ng/mL vascular endothelial growth factor; all from R&D Systems) for 2 d and then

cultured in MSC media with or without cytokine for 10 d. To investigate the reprogramming cell-signaling pathways, inhibitors were added to the reprogramming mixture from day 1 and kept for 12 d. Media was refreshed every 3–4 d. At the end of day 12, cells were harvested for downstream analysis.

Reprogramming primary mouse osteocytes. FACS-sorted long-bone–derived SCA1$^-$/CD31$^-$/PDGFRA$^-$/DMP1eYFP$^+$ primary osteocytes were cultured on type I rat tails in collagen-coated 35 mm^2 dishes in the osteocyte culture medium (αMEM + 5% FCS + P/S/G) for 3 d. On day 4, osteocyte culture media was replaced with reprogramming media (αMEM + 20% FCS + 100 ng/mL mouse recombinant PDGF-AB + 10 μM AZA + P/S/G) and cultured for a further 48 h. At the end of 48 h, reprogramming media was replaced with αMEM + 20% FCS + 100 ng/mL mouse recombinant PDGF-AB + P/S/G media and cultured for a further 10 d with every 3 d media change. On day 12, reprogrammed cells were harvested for characterization.

Reprogramming primary mouse adipocytes. Harvested primary adipocytes were cultured in adipocyte medium for 8–10 days. Reprogramming media [αMEM + 20% (vol/vol) FCS + 100 ng/mL mouse recombinant PDGF-AB + 10 μM AZA + P/S/G] was added on day 11 and cultured for further 48 h. At the end of 48 h, reprogramming media was replaced with αMEM + 20% FCS + 100 ng/mL mouse recombinant PDGF-AB + P/S/G media and cultured for another 10 d with every 3 d media change. On day 12, reprogrammed cells were harvested for characterization.

Reprogramming primary human adipocytes. S.c. fat was harvested with consent from patients undergoing surgery for degenerative disk disease with approval from the Prince of Wales Hospital human research ethics committee. The s.c. adipocytes were harvested using a previously described method (45) with modifications (see *SI Appendix*). Harvested primary human adipocytes were exposed to reprogramming media containing 10 μM AZA + 200 ng/mL human recombinant PDGF-AB + 20% autologous serum + P/S/G for 2 d and then maintained in 200 ng/mL human recombinant PDGF-AB + 20% autologous serum + P/S/G for a further 23 d with every 3–4 d media change. On day 25, reprogrammed adipocytes were harvested for characterization.

Inhibitor Assays. To investigate the reprogramming of cell signaling pathways, inhibitors were added to the reprogramming mixture from day 1 and kept for 12 d. Media was refreshed every 3–4 d. At the end of day 12, cells were harvested for downstream analysis (see *SI Appendix*).

Live Cell Imaging. Cells were imaged using an IncuCyte microscope (Essen Bioscience) with 10× phase objective and a Nikon Ti-E microscope with a 20× phase objective (0.45 N.A.). Images were captured every 60 and 30 min, respectively, for 8 d (see *SI Appendix*).

CFU-F Long-Term Growth and Serial Clonogenicity. For details on CFU-F long-term growth and serial clonogenicity, see *SI Appendix*.

In Vitro Lineage Differentiation. Reprogrammed cells were differentiated into derivatives of all three germ layers as detailed in *SI Appendix*.

Teratoma Formation. Rag1 mice were injected (under the kidney capsule) with mouse HM1 ES cells (n = 2) or CFU-Fs (n = 3), osteocytes (n = 3), and oCFU-Fs (n = 3) from β2-microglobulin-GFP mice either alone or as a mixture of mESCs and CFU-Fs (n = 3), osteocytes (n = 3), or oCFU-Fs (n = 3) (mESCs:cells, 1:3) (see *SI Appendix*).

Immunohistochemistry. All antibodies and methods are listed in *SI Appendix*.

Gene Expression and Epigenetic Analyses. All primers are listed under *SI Appendix*. High-quality RNA was profiled using Illumina's Mouse WG-6 v2.0 Bead arrays and analyzed as detailed in *SI Appendix*. Allelic bisulphite sequencing and NOMe-Seq were performed as detailed in *SI Appendix*. Expression data have been deposited in the Gene Expression Omnibus under accession no. GSE59282.

Posterior–Lateral Intertransverse Lumber Fusion Model. Long bones were harvested from either β2-microglobulin-GFP or DMP1eYFP mice; soft tissues were removed, flushed out, fragmented, and collagenase-treated; and the supernatant was discarded. Either bone fragments or DMP1eYFP$^+$ osteocytes were cultured in reprogramming or control media for 12 d and surgically implanted into the posterior–lateral lumbar spine region (L4–L5) in Rag1 mice. At 6 and 12 wk, mice were euthanized and analyzed as detailed in *SI Appendix*.

ACKNOWLEDGMENTS. The authors thank Dr. C. Glenn Begley and Dr. Jose Polo for reading and commenting on the manuscript. This work was supported by grants from the National Health and Medical Research Council of Australia and the Australian Research Council. A.Y. was supported by an Endeavour Scholarship from the Australian Government.

1. Thomas ED, Lochte HL, Jr, Lu WC, Ferrebee JW (1957) Intravenous infusion of bone marrow in patients receiving radiation and chemotherapy. *N Engl J Med* 257(11):491–496.
2. Hauben DJ, Baruchin A, Mahler A (1982) On the history of the free skin graft. *Ann Plast Surg* 9(3):242–245.
3. Donati D, Zolezzi C, Tomba P, Viganò A (2007) Bone grafting: Historical and conceptual review, starting with an old manuscript by Vittorio Putti. *Acta Orthop* 78(1):19–25.
4. Sandler VM, et al. (2014) Reprogramming human endothelial cells to haematopoietic cells requires vascular induction. *Nature* 511(7509):312–318.
5. Bianco P, et al. (2013) The meaning, the sense and the significance: Translating the science of mesenchymal stem cells into medicine. *Nat Med* 19(1):35–42.
6. Wilmut I, Schnieke AE, McWhir J, Kind AJ, Campbell KH (1997) Viable offspring derived from fetal and adult mammalian cells. *Nature* 385(6619):810–813.
7. Cowan CA, Atienza J, Melton DA, Eggan K (2005) Nuclear reprogramming of somatic cells after fusion with human embryonic stem cells. *Science* 309(5739):1369–1373.
8. Tada M, Takahama Y, Abe K, Nakatsuji N, Tada T (2001) Nuclear reprogramming of somatic cells by in vitro hybridization with ES cells. *Curr Biol* 11(19):1553–1558.
9. Takahashi K, Yamanaka S (2006) Induction of pluripotent stem cells from mouse embryonic and adult fibroblast cultures by defined factors. *Cell* 126(4):663–676.
10. Yamanaka S, Blau HM (2010) Nuclear reprogramming to a pluripotent state by three approaches. *Nature* 465(7299):704–712.
11. Vierbuchen T, et al. (2010) Direct conversion of fibroblasts to functional neurons by defined factors. *Nature* 463(7284):1035–1041.
12. Zhou Q, Brown J, Kanarek A, Rajagopal J, Melton DA (2008) In vivo reprogramming of adult pancreatic exocrine cells to beta-cells. *Nature* 455(7213):627–632.
13. Sekiya S, Suzuki A (2011) Direct conversion of mouse fibroblasts to hepatocyte-like cells by defined factors. *Nature* 475(7356):390–393.
14. Ieda M, et al. (2010) Direct reprogramming of fibroblasts into functional cardiomyocytes by defined factors. *Cell* 142(3):375–386.
15. Riddell J, et al. (2014) Reprogramming committed murine blood cells to induced hematopoietic stem cells with defined factors. *Cell* 157(3):549–564.
16. Pereira CF, et al. (2013) Induction of a hemogenic program in mouse fibroblasts. *Cell Stem Cell* 13(2):205–218.
17. Fu JD, et al. (2013) Direct reprogramming of human fibroblasts toward a cardiomyocyte-like state. *Stem Cell Rep* 1(3):235–247.
18. Wallace H (1981) *Vertebrate Limb Regeneration* (Wiley, Chichester, UK).
19. Hemberger M, Dean W, Reik W (2009) Epigenetic dynamics of stem cells and cell lineage commitment: Digging Waddington's canal. *Nat Rev Mol Cell Biol* 10(8):526–537.
20. Silverman LR, Mufti GJ (2005) Methylation inhibitor therapy in the treatment of myelodysplastic syndrome. *Nat Clin Pract Oncol* 2(Suppl 1):S12–S23.
21. Jones PA, Taylor SM (1980) Cellular differentiation, cytidine analogs and DNA methylation. *Cell* 20(1):85–93.
22. Taylor SM, Jones PA (1979) Multiple new phenotypes induced in 10T1/2 and 3T3 cells treated with 5-azacytidine. *Cell* 17(4):771–779.
23. Nixon BT, Green H (1984) Growth hormone promotes the differentiation of myoblasts and preadipocytes generated by azacytidine treatment of 10T1/2 cells. *Proc Natl Acad Sci USA* 81(11):3429–3432.
24. Locklin RM, Oreffo RO, Triffitt JT (1998) Modulation of osteogenic differentiation in human skeletal cells in vitro by 5-azacytidine. *Cell Biol Int* 22(3):207–215.
25. Makino S, et al. (1999) Cardiomyocytes can be generated from marrow stromal cells in vitro. *J Clin Invest* 103(5):697–705.
26. Pennarossa G, et al. (2013) Brief demethylation step allows the conversion of adult human skin fibroblasts into insulin-secreting cells. *Proc Natl Acad Sci USA* 110(22):8948–8953.
27. Mikkelsen TS, et al. (2008) Dissecting direct reprogramming through integrative genomic analysis. *Nature* 454(7200):49–55.
28. Semerad CL, et al. (2005) G-CSF potently inhibits osteoblast activity and CXCL12 mRNA expression in the bone marrow. *Blood* 106(9):3020–3027.
29. Hamilton TG, Klinghoffer RA, Corrin PD, Soriano P (2003) Evolutionary divergence of platelet-derived growth factor alpha receptor signaling mechanisms. *Mol Cell Biol* 23(11):4013–4025.
30. Morikawa S, et al. (2009) Prospective identification, isolation, and systemic transplantation of multipotent mesenchymal stem cells in murine bone marrow. *J Exp Med* 206(11):2483–2496.
31. Lu Y, et al. (2007) DMP1-targeted Cre expression in odontoblasts and osteocytes. *J Dent Res* 86(4):320–325.
32. Rao RD, Bagaria VB, Cooley BC (2007) Posterolateral intertransverse lumbar fusion in a mouse model: Surgical anatomy and operative technique. *Spine J* 7(1):61–67.
33. Schaefer BC, Schaefer ML, Kappler JW, Marrack P, Kedl RM (2001) Observation of antigen-dependent CD8+ T-cell/dendritic cell interactions in vivo. *Cell Immunol* 214(2):110–122.
34. Yagi H, et al. (2010) Mesenchymal stem cells: Mechanisms of immunomodulation and homing. *Cell Transplant* 19(6):667–679.
35. Jones PA (2012) Functions of DNA methylation: Islands, start sites, gene bodies and beyond. *Nat Rev Genet* 13(7):484–492.
36. Kelly TK, et al. (2010) H2A.Z maintenance during mitosis reveals nucleosome shifting on mitotically silenced genes. *Mol Cell* 39(6):901–911.

37. Karsenty G (2008) Transcriptional control of skeletogenesis. *Annu Rev Genomics Hum Genet* 9:183–196.
38. Stresemann C, Lyko F (2008) Modes of action of the DNA methyltransferase inhibitors azacytidine and decitabine. *Int J Cancer* 123(1):8–13.
39. Marcucci G, Silverman L, Eller M, Lintz L, Beach CL (2005) Bioavailability of azacitidine subcutaneous versus intravenous in patients with the myelodysplastic syndromes. *J Clin Pharmacol* 45(5):597–602.
40. Hoch RV, Soriano P (2003) Roles of PDGF in animal development. *Development* 130(20):4769–4784.
41. Heldin CH, et al. (1985) Platelet-derived growth factor: Mechanism of action and relation to oncogenes. *J Cell Sci Suppl* 3:65–76.
42. Heldin CH, Westermark B (1990) Platelet-derived growth factor: Mechanism of action and possible in vivo function. *Cell Regul* 1(8):555–566.
43. Radzisheuskaya A, Silva JC (2014) Do all roads lead to Oct4? The emerging concepts of induced pluripotency. *Trends Cell Biol* 24(5):275–284.
44. Marson A, et al. (2008) Connecting microRNA genes to the core transcriptional regulatory circuitry of embryonic stem cells. *Cell* 134(3):521–533.
45. Fernyhough ME, et al. (2004) Primary adipocyte culture: Adipocyte purification methods may lead to a new understanding of adipose tissue growth and development. *Cytotechnology* 46(2-3):163–172.
46. Chong JJ, et al. (2011) Adult cardiac-resident MSC-like stem cells with a proepicardial origin. *Cell Stem Cell* 9(6):527–540.